AJNR

Functional MR in the evaluation of dementia: correlation of abnormal dynamic cerebral blood volume measurements with changes in cerebral metabolism on positron emission tomography with fludeoxyglucose F 18.

R G GonzÖ°lez, A J Fischman, A R Guimaraes, C A Carr, C E Stern, E F Halpern, J H Growdon and B R Rosen

AJNR Am J Neuroradiol 1995, 16 (9) 1763-1770
http://www.ajnr.org/content/16/9/1763

Functional MR in the Evaluation of Dementia: Correlation of Abnormal Dynamic Cerebral Blood Volume Measurements with Changes in Cerebral Metabolism on Positron Emission Tomography with Fludeoxyglucose F 18

R. Gilberto González, Alan J. Fischman, Alexander R. Guimaraes, Cindy A. Carr, Chantal E. Stern, Elkan F. Halpern, John H. Growdon, and Bruce R. Rosen

PURPOSE: To determine whether magnetic susceptibility functional MR imaging of cerebral blood volumes provides information similar to fludeoxyglucose F 18 positron emission tomography (PET) brain images in patients undergoing evaluation for dementia. **METHODS:** Ten subjects were studied with both PET and functional MR. Clinical diagnoses included probable Alzheimer disease (n = 5), possible Alzheimer disease (n = 1), Pick disease (n = 2), and primary progressive aphasia (n = 2). The studies were quantitatively evaluated by coregistration of PET and functional MR images followed by regression analyses of corresponding regions of interest. Qualitatively, each brain was categorized into eight regions, and each was classified as normal or abnormal by visual inspection. **RESULTS:** Correlation coefficients between registered functional MR and PET images were excellent (mean, $r = 0.58$) in most of the cerebrum. Significant correlations were observed in 72 of 74 brain sections. Qualitatively, 16 brain regions were judged to be abnormal by both MR imaging and PET; 46 regions were normal by both; 10 regions were abnormal by PET only; and 8 regions were abnormal only by functional MR. The concordance between functional MR and PET was 78%, which was highly significant. **CONCLUSION:** Cerebral blood volumes images derived from magnetic susceptibility (functional MR) provide information similar to fludeoxyglucose F 18 PET images in demented patients undergoing evaluation for dementia.

Index terms: Dementia; Magnetic resonance, functional; Positron emission tomography

AJNR Am J Neuroradiol 16:1763–1770, October 1995

The purpose of this study was to examine the potential use of functional magnetic resonance (MR) in the evaluation of patients with clinical evidence of dementia. Currently, the diagnostic assessment of dementia includes computed tomography (CT) or MR of the brain. These methods are primarily used to exclude dementing syndromes attributable to infarcts, hydrocephalus, and neoplasms. Standard imaging does not detect structural change of the brain that are specific for the diagnosis of Alzheimer disease (AD), which is the most common cause of dementia. Quantitative measurements of medial temporal lobe structures have been reported to define statistical differences between AD and other types of dementia (1–4) but have not yet achieved widespread validation and application.

Cognitive tests can demonstrate evidence of dementia, such as impaired memory and language deficits, even when the brain CT or MR study appears intact for age. Because of this observation, physiologic measurements of the brain have been devised to assess brain function. Studies using positron emission tomography (PET) and single-photon emission CT

Received December 22, 1994; accepted after revision May 17, 1995.

Supported by US Public Health Service Grant AG10679.

From the Massachusetts General Hospital NMR Center (R.G.G., A.R.G., C.A.C., C.E.S., B.R.R.) and Center for Imaging and Pharmaceutical Research (E.F.H.), Department of Radiology, Massachusetts General Hospital, Harvard Medical School, Charlestown; and the Neuroradiology Division (R.G.G.) and the MGH PET Laboratory (A.J.F.), Department of Radiology, and Massachusetts Alzheimer's Disease Research Center (J.H.G.), Department of Neurology, Massachusetts General Hospital, Harvard Medical School, Boston.

Address reprint requests to Gilberto González, MGH NMR Center, Bldg 149, 13th St, 2nd Fl, Rm 2301, Charlestown, MA 02129.

AJNR 16:1763–1770, Oct 1995 0195-6108/95/1609–1763

(SPECT) have been shown to be superior to routine anatomic CT and MR in differentiating AD from other causes of dementia. PET (5–7) and SPECT (8) have proved capable of demonstrating regional deficits in metabolism and perfusion in AD. For this reason, they often are used in the assessment of dementing syndromes.

Functional MR recently has emerged as a new method that may provide information similar to that from SPECT and PET. The MR data needed to generate a functional brain image may be acquired rapidly. This raises the possibility that functional MR may be performed during routine MR studies of patients undergoing evaluation for symptoms of dementia. To assess the potential value of functional MR, it is important to validate functional MR with another functional technique. In this study, we test the hypothesis that dynamic cerebral blood volume images derived from magnetic susceptibility functional MR obtained during the first pass of intravenously injected paramagnetic contrast agent provide information similar to information from fludeoxyglucose F 18 (FDG) PET studies in patients with dementia.

Methods

We studied 10 patients with dementia who were referred from the Memory Disorders Unit of our hospital. The mean age ± SD of our sample group was 70.3 ± 9.4 years (range, 54 to 83 years). Inclusion criteria for the study included confirmation of one or more cognitive deficits by the clinical and neuropsychological methods of the Memory Disorders Unit and the capability of undergoing MR and PET imaging within a 2-week period. The standard MR exclusion criteria, such as the presence of a pacemaker, were used. Diagnoses were established based on routine clinical criteria and were made independent of findings in this research study. We anticipated that some would have global deficits (probable AD [n = 5]; possible AD [n = 1]), and others would have focal deficits (primary progressive aphasia [n = 2] and probable Pick disease [n = 2]). The study was approved by the institutional review board. All patients signed consent forms.

PET scans were performed using FDG. Typically, between 200 and 300 MBq of FDG was injected intravenously. Approximately 45 minutes after injection of the radiopharmaceutical agent, PET scans of the brain were obtained. Between injection and the scan, the patients were kept in the patient waiting area, and no special instructions were given. The waiting room was well lit and usually contained several patients. Of the 10 studies, 7 were performed on Scandatronics PC-384 camera and 3 on the PC-4096 cameras.

For the MR study, the patient was positioned within a 1.5-T magnet and routine sagittal T1-weighted and axial T2-weighted images of the brain were obtained. Functional MR studies were performed using an echo planar imaging system as previously described by Aronen et al (9). Shimming was performed before the cerebral blood volume imaging scan to ensure optimal signal to noise. The parameters for the echo planar imaging pulse sequence were: 1500/100/1 (repetition time/echo time/excitations); field of view, 20 × 40 cm; matrix size, 128 × 256; section thickness, 7 mm skip 7 mm; 8 sections; 64 images per section; and a temporal resolution of 1.5 seconds for each section. The sections were prescribed from the posterior fossa to the brain convexity by using a scout sagittal midline image. The data acquisition for the dynamic cerebral blood volume MR scan lasted 1:43 minutes and was collected at the rate of eight images per 1.5 seconds. Patients were injected with 0.2 mmol/kg gadopentetate dimeglumine (5 mL/s) by a power injector 15 seconds after data acquisition had commenced. Before the bolus gadopentetate dimeglumine injection, approximately 10 images per section were acquired, which were used as baseline data for the calculation of the cerebral blood volume images.

Dynamic cerebral blood volume images were generated using a computer algorithm developed in our laboratory. The algorithm uses the principles of tracer kinetic and susceptibility-contrast MR (9–12). Initially, the algorithm plots the signal intensity as a function of time for each voxel. A ΔR2 transformation is then performed, which results in a plot of contrast agent tissue concentration versus time for each voxel. ΔR2 is related to the T2 change ($\Delta(1/T2^*)=\Delta R2$) at a given echo time and is dependent on the brain tissue contrast concentration. This relationship previously has been described (9–12) and is defined in equation 1:

$$1) \qquad \Delta R2 = k[conc]$$

where [conc] is the brain tissue contrast concentration, and k is a tissue, pulse sequence, and field strength–specific constant. The change in signal intensity pursuant to the bolus contrast injection is used to derive the concentration-time curve using equation 2, as has been previously described (9–12):

$$2) \qquad -\ln(S(t)/So/TE) = k[conc.(t)]$$

where So is the baseline signal intensity before injection, S(t) is the tissue signal with contrast agent present, and TE is the echo time. The ΔR2 vs time curve for each voxel then is used to calculate the relative cerebral blood volume for that voxel: an integration is performed over the region where the curve deviates from the baseline, reflecting the beginning of the passage of contrast through the brain and when the curve returns to its baseline as the contrast finishes its passage. The algorithm smoothes each section

using a 3×3-pixel kernel. The kernel calculates the mean of the squares of the target pixel and the eight surrounding pixels and replaces the initial target pixel value with this mean value. As a result of this analysis, the signal intensity of each pixel is directly related to the relative cerebral blood volume within the image plane.

To compare PET and functional MR quantitatively, the images were coregistered. We used a program developed at our laboratory for this purpose. Dynamic cerebral blood volume images, T2-weighted axial images, and FDG PET images were needed to perform the coregistration. Each cerebral blood volume image had a matching image in the T2-weighted axial set. Because the T2-weighted image set more completely encompassed the entire brain, the PET images were registered to these. Modification of the PET images was accomplished by the application of a transformation matrix, which was derived by manipulating translations in three orthogonal directions and three rotational angles. The transformation matrix was applied to the original PET data after each of the translational and rotational variables had been adjusted to minimize the misalignment between the MR axial and PET images. The PET images were subsequently reformatted by using a trilinear interpolation to calculate the intensity of each voxel in the new PET image data set.

To compute the correlation coefficients between corresponding PET and relative cerebral blood volume images, we made pixel comparisons from two-dimensional image displays of the reregistered PET data versus the corresponding two-dimensional calculated regional cerebral blood volume image. Corresponding 7×7-pixel regions of interest from the relative cerebral blood volume and PET images were plotted in two-dimensional graphs of relative cerebral blood volume versus PET signal intensities. Several hundred data points were generated from each corresponding section. Linear regression and Pearson r correlation statistical tools were used to determine significance of correlations between corresponding PET and relative cerebral blood volume images.

For the qualitative part of the study, the original unregistered PET and functional MR images were visually inspected. Judgments of normality or abnormality were made on eight brain regions: frontal, parietal/posterior temporal, anterior temporal, and occipital regions of the right and left hemispheres. The parietal and posterior temporal regions were combined because of the difficulty in differentiating these regions on the MR axial images of varying obliquity. The PET scans were reviewed by two physicians who perform clinical interpretations of PET brain scans. Normal metabolic activity or abnormal metabolic deficits for each region of brain was determined by consensus between the two readers. The functional MR cerebral blood volume maps were interpreted qualitatively by two individuals experienced in the interpretation of these images. The normality or abnormality of blood volume in each region of brain also was determined by consensus. The functional MR studies were interpreted independently from the PET scans in a blinded fashion. Statistical analysis was performed using the standard χ^2 method to test the hypothesis of no relationship. Concordance was expressed in terms of κ.

Results

Quantitative comparisons between the functional MR and PET scans were undertaken after coregistration of the images for each subject. The functional MR studies produced fewer images per brain, and, therefore, the PET scans were registered and resectioned to match the functional MR scans. An example of a functional MR cerebral blood volume image and the corresponding registered PET image at the same level are shown in Figure 1. A plot of the values of the spatially corresponding pixels from these images is shown in Figure 2. In this case, a high correlation coefficient ($r = 0.73$; $n = 408$) of high significance ($P < 10^{-12}$) was observed.

A summary of the results from all of the brain images is shown in Figure 3 and the Table. High correlation coefficients were consistently observed in the brain images of the paraventricular and supraventricular regions of the cerebrum. Lower correlations were observed in the temporal lobe and posterior fossa regions. Nonetheless, statistically significant correlations were observed in 72 of 74 brain sections. As discussed below, we believe that artifacts arising from the functional MR method are the cause of the lower correlations observed in the lower brain sections.

For the qualitative part of this study, the brain images from each subject were categorized into eight regions, and each region was judged to be either normal or abnormal by visual inspection of the PET or functional MR images. Of 80 separate brain regions that were evaluated, 16 were found to be abnormal on both MR and PET, and 46 locations were normal on both examinations. Ten regions were judged abnormal by PET only, and 8 regions were considered to be abnormal by functional MR only. The P value from the χ^2 test of the hypothesis of no association between PET and functional MR was .0001. Hence, we reject this hypothesis and conclude that the judgments of normality based on functional MR and PET are associated. Overall agreement between the methods was approximately 78%. This yielded a κ of .702.

Examples of brain images with concordant normal and abnormal regions are shown in Figure 4. These images were obtained from an

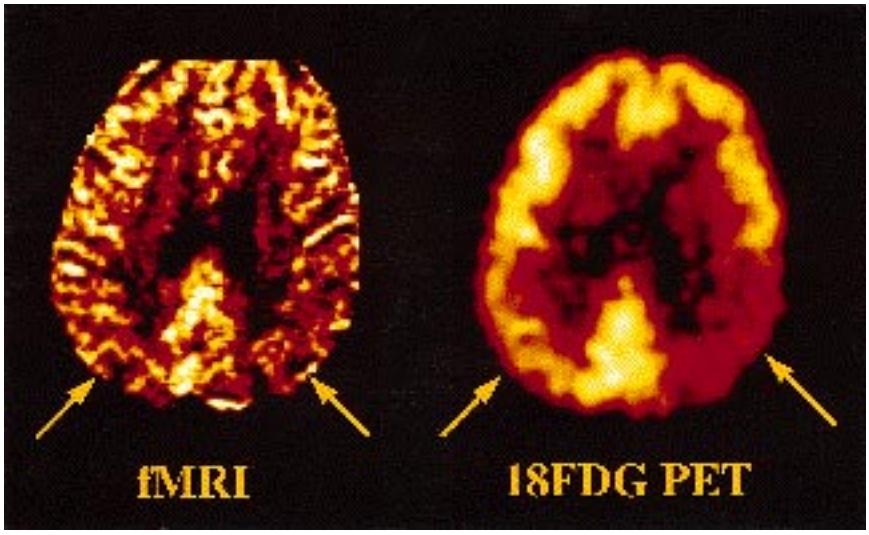

Fig 1. Dynamic cerebral blood volume image derived using magnetic susceptibility functional MR (*left*) and FDG PET image (*right*) at the same level from a patient. The PET images were registered to the functional MR images and sectioned to give matching brain images. In the color scale, areas of higher blood volume and glucose metabolism appear yellow, whereas lower relative values of these parameters appear red. In this subject with probable Alzheimer disease, there is a corresponding decrease in glucose metabolism and dynamic blood volumes in the parietal lobes (*arrows*). The deficits appear worse on the left side.

individual with a clinical diagnosis of probable AD. This patient had glucose metabolic deficits in the parietal lobes that were worse on the left side. The functional MR cerebral blood volume image is remarkable for the decreased blood volume seen bilaterally in the parietal lobes and is more pronounced on the left. As in this example, brain regions with areas of substantially decreased metabolism revealed by PET usually had a corresponding decrease in cerebral blood volume by functional MR. Metabolic asymmetries were commonly observed. When such asymmetries were detected, a similar asymmetry usually was detected in the functional MR cerebral blood volume map of that region.

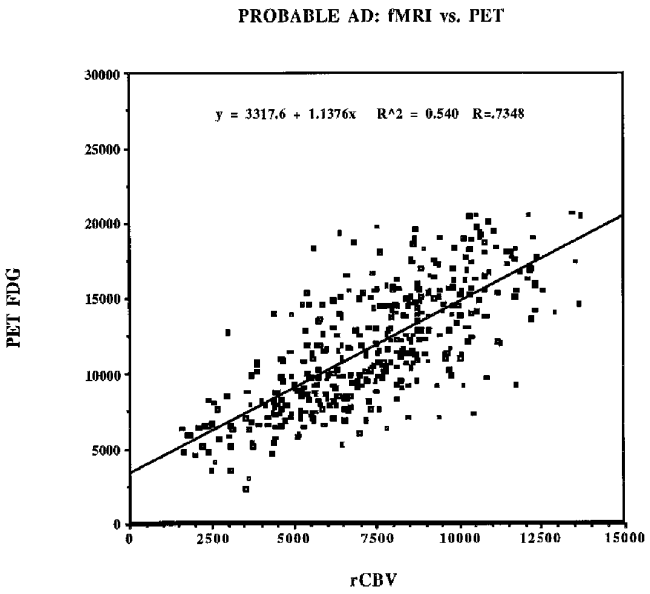

Fig 2. Plot of the FDG PET (*vertical axis*) versus the functional MR (*horizontal axis*) of matching pixel intensities of the images shown in Figure 1. The plot was created after the registration of cerebral blood volume and PET images as described in "Methods." The correlation coefficient for this brain section was high ($r = 0.73$) and highly significant ($P < 10^{-12}$).

There were occasional disagreements between the functional MR cerebral blood volume and the FDG PET images. These usually occurred with small focal areas of hypometabolism that were detected on PET without a corresponding visually detected abnormality on the functional MR image. However, on rare occasions, a substantial area of diminished metabolism detected by PET was not detected by functional MR. We reviewed the baseline MR images to investigate whether focal abnormalities could explain the observed discordance. Although several subjects had focal white matter abnormalities, they did not explain the discordant findings. Further studies will be required to learn more clearly when and why such disagreements in PET and functional MR measurements occur.

Two PET cameras were used. The resolution of the PC-384 camera is 7 × 7 mm (full width at half maximum) with a section thickness of 12 mm. The PC-4096 camera has a resolution of

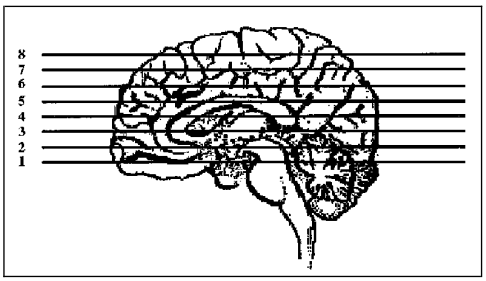

Fig 3. Figure 3 depicts the approximate center of each individual section (also see the Table).

Correlations between functional MR cerebral blood volume and FDG PET brain sections

Section	Location	Average *r*	Average *P* Value for Each Correlation
8	Convexity	0.41	$<10^{-11}$
7	Supraventricular	0.53	$<10^{-12}$
6	Supraventricular	0.62	$<10^{-12}$
5	Paraventricular	0.62	$<10^{-12}$
4	Paraventricular	0.57	$<10^{-12}$
3	High temporal	0.33	$<10^{-12}$
2	Low temporal	0.24	$<10^{-6}$
1	Posterior fossa	0.26	$<10^{-5}$

6 × 6 mm with a section thickness of 6 mm. The three studies that were performed on the high-resolution camera had a higher concordance (>90%) on the qualitative studies and higher than the average correlation coefficients for each brain section level.

This preliminary study was designed to compare the functional MR cerebral blood volume images with FDG PET images in the same individual. No attempt was made to assess the sensitivity or specificity of functional MR relative to PET in the diagnosis of AD or other diseases. We note, however, that the majority of the patients with the diagnosis of probable or possible AD had parietal/posterior temporal abnormalities bilaterally. The two patients with clinical diagnoses of Pick disease had frontal lobe and anterior temporal lobe abnormalities that were detected by one or both methods.

Discussion

In our study of patients under evaluation for dementia, we found that quantitative and qualitative comparisons of images of brain dynamic cerebral blood volume obtained by functional MR and FDG PET were highly correlated and highly statistically significant. This finding supports the hypothesis that magnetic susceptibility functional MR provides brain functional information similar to that from FDG PET in patients under evaluation for dementia.

When we compared functional MR and FDG PET studies quantitatively, we noted high correlation coefficients in the paraventricular and supraventricular regions of the brain (Table). The correlation coefficients (*r*) in these brain regions averaged ~0.6. This finding compares very favorably with reported correlation coefficients observed for scans obtained in the same individuals in an earlier PET investigation. In an investigation by Duara and colleagues, nine healthy subjects and four demented subjects were imaged twice by using FDG PET at intervals ranging from 1 to 6 weeks (13). They reported a correlation coefficient of 0.7 between images of the same subject. The degree of agreement that we find between the functional MR and PET images is notable, because the subjects may have had different brain activation states during each examination. For instance, in the PET study, patients were sitting in a lit room with other people, reading, conversing, or sitting quietly during the 45-minute interval between the FDG injection and scanning. These activities may have affected precise glucose uptake patterns. By contrast, in the functional MR study, patients were lying within a darkened and noisy magnet.

Although the correlation coefficients between functional MR and PET are high in the regions of the central cerebrum, they are substantially lower in the posterior fossa and region of the temporal lobes. The most likely explanation for this observation is that the echo planar imaging method used for functional MR generates a substantial amount of artifact in the latter regions (see Fig 4A), thus introducing errors in the cerebral blood volume image calculations. For example, in Figure 4, there are marked pulsation artifacts in the middle cranial fossa caused by the middle cerebral artery. We believe that magnetic susceptibility artifacts also are responsible for the relatively low correlation coefficients found in the posterior fossa. Nevertheless, correlations with high statistical significance were observed in 72 brain sections of the 74 compared.

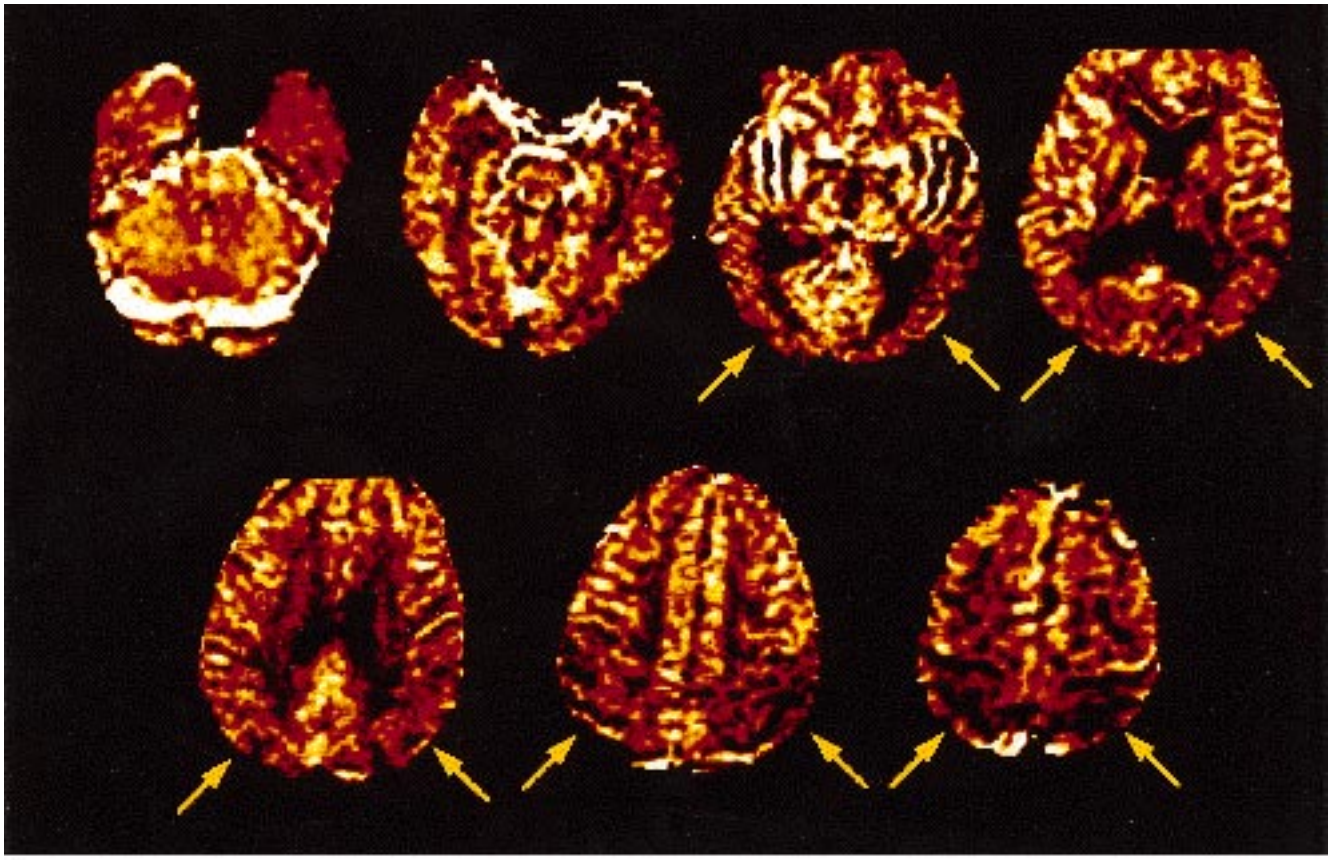

A

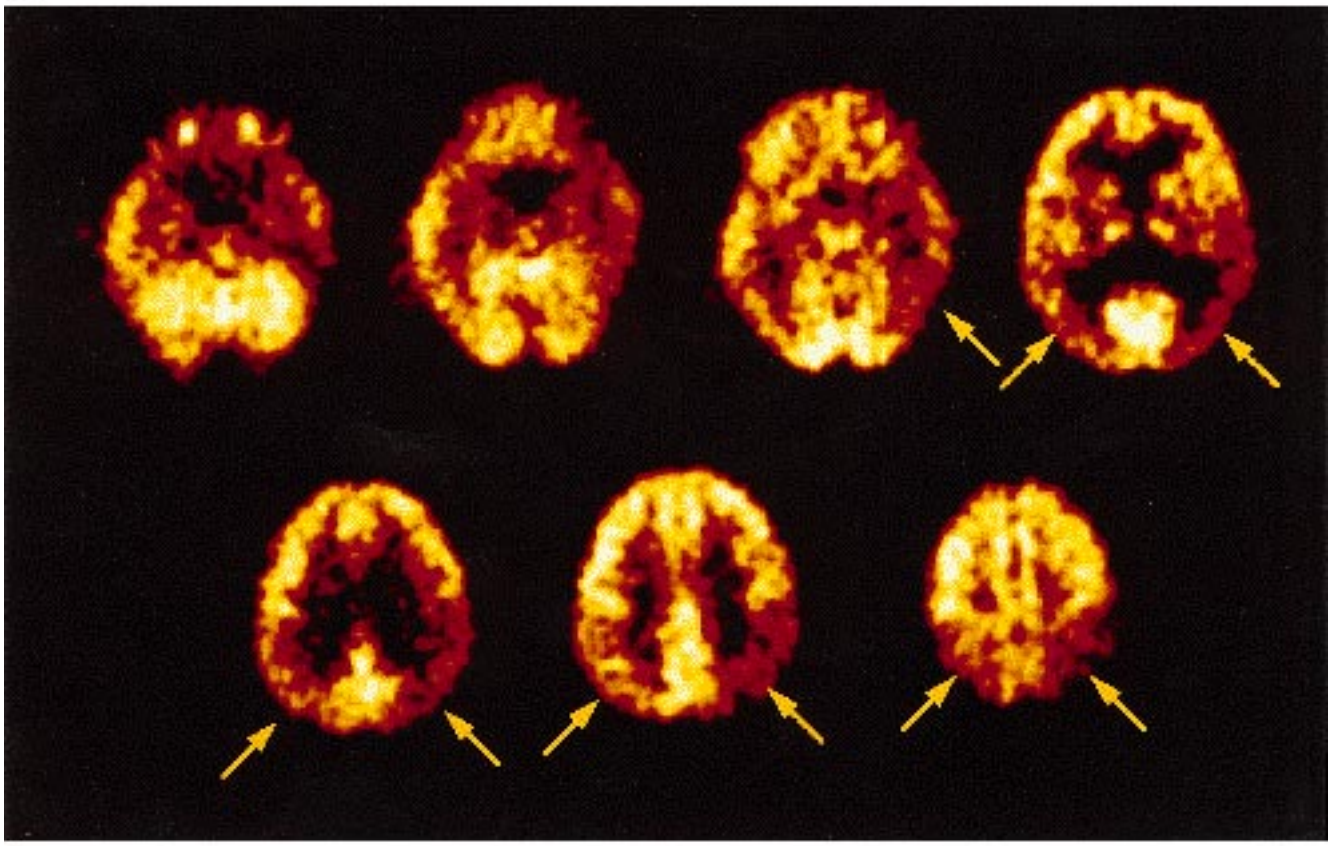

B

In our qualitative comparison of the functional MR and PET studies, we found a strong concordance of approximately 78% between the images ($\kappa = 0.702$). Areas in which we observed decreased glucose metabolism generally corresponded to areas of decreased blood volumes. Disagreements between the functional MR and PET readings usually occurred in small areas of abnormal cerebral blood volume or abnormal glucose metabolism. On one occasion, however, a relatively large area of abnormal glucose metabolism was not detected in the cerebral blood volume image. An explanation for this observation will require further study.

We observe a high concordance between regional metabolism and regional blood volumes. This observation is consistent with previous studies performed under a variety of circumstances. Regions of high metabolic activity will increase local delivery of oxygen and nutrients through increased blood flow, as first postulated by Roy and Sherrington (14). The coupling of cerebral blood flow with neuronal activity has been amply demonstrated in animal studies (15). The coupling of regional cerebral blood flow with regional cerebral metabolic rate in higher animals also has been demonstrated (16, 17), although the relationship may not be linear (18). Finally, a linear relationship between regional cerebral blood flow and regional cerebral blood volume has been shown over a substantial range in humans (18, 19). Thus, we expected to find a relationship between relative cerebral blood volume and regional cerebral metabolism.

A correlation between PET regional cerebral glucose metabolism and functional MR regional cerebral blood volume has been noted in other studies performed in our laboratory. For example, studies of brain neoplasms (9, 12) have shown that increased cerebral blood volume correlates highly with increased metabolic activity as detected by PET. In studies of brain function in response to visual stimulation, a focal increase in blood volume was observed after stimulation of the appropriate regions of the visual cortex (11). Visual stimulation also is known to cause increased metabolic activity in the primary visual cortex.

Our results suggest that dynamic cerebral blood volume images derived from functional MR provide information similar to that from other neuroimaging techniques, such as PET or SPECT, which measure brain function and are thus of use in the study of AD. The clinical value of functional MR in helping to differentiate AD from other dementing processing will require further research, which we have commenced. Another related outstanding question is whether functional MR can measure the progression of AD and thereby aid in the evaluation of potential AD therapies. Were functional MR to prove useful in these, the technique's usefulness in the diagnosis and potentially in the treatment of AD would be great. This is especially the case because functional MR data are acquired rapidly and can be incorporated easily into a standard brain MR examination. Thus, magnetic susceptibility functional MR may be an important new technique for investigations of AD and other dementias.

Fig 4. Cerebral blood volume images derived using functional MR (*A*) and selected corresponding FDG PET images (*B*) from the same individual with a clinical diagnosis of probable Alzheimer disease. Registration was not performed on these images. Asymmetric, diminished glucose uptake in the parietal lobes is matched by decreased relative blood volumes in the same regions (*arrows*).

References

1. Kesslak J, Nalcioglu O, Cotman C. Quantification of magnetic resonance scans for hippocampal and parahippocampal atrophy. *Neurology* 1991;41:51–54
2. Jack C, Petersen R, O'Brien P, Tangalos E. MR-based hippocampal volumetry in the diagnosis of Alzheimer's disease. *Neurology* 1992;42:183–188
3. Killiany R, Moss M, Albert M, Sandor T, Tieman J, Jolesz F. Temporal lobe regions on magnetic resonance imaging identify patients with early Alzheimer's disease. *Arch Neurol* 1993;50: 949–954
4. Lehérciy S, Baulac M, Chiras J, et al. Amygdalohippocampal MR volume measurements in the early stages of Alzheimer disease. *AJNR Am J Neuroradiol* 1994;15:929–937
5. Frackowiak R, Pozzilli C, Legg N, et al. Regional cerebral oxygen supply and utilization in dementia: a clinical and physiological study with oxygen-15 and positron tomography. *Brain* 1981;104: 753–778
6. Benson D, Kuhl D, Hakins R, Phelps M, Cummings J, Tsai S. The fluorodeoxyglucose 18F scan in Alzheimer's disease and multi-infarct dementia. *Arch Neurol* 1983;40:711–714
7. Rapoport S. Positron emission tomography in Alzheimer's disease in relation to disease pathogenesis: a critical review. *Cerebrovasc Brain Metab Rev* 1991;3:297–335
8. Johnson K, Holman B, Rosen T, Nagel J, English R, Growdon J. Iofetamine I 123 single photon emission computed tomography is accurate in the diagnosis of Alzheimer's disease. *Arch Intern Med* 1990;150:752–756

9. Aronen H, Gazit I, Louis D, et al. Cerebral blood volume maps of gliomas: comparison with tumor grade and histologic findings. *Radiology* 1994;191:41–51
10. Belliveau JW, Rosen BR, Kantor HL, et al. Functional cerebral imaging by susceptibility-contrast NMR. *Magn Reson Med* 1990; 14:538–546
11. Belliveau J, Kennedy D, McKinstry R, et al. Functional mapping of the human visual cortex by magnetic resonance imaging. *Science* 1991;254:716–719
12. Aronen H, Cohen M, Belliveau J, Fordham J, Rosen B. Ultrafast imaging of brain tumors. *Top Magn Reson Imaging* 1993;5:14–24
13. Duara R, Gross-Glenn K, Barker W, et al. Behavioral activation and the variability of cerebral glucose metabolic measurements. *J Cereb Blood Flow Metab* 1987;7:266–271
14. Roy C, Sherrington C. On the regulation of the blood-supply of the brain. *J Physiol* 1890;11:85–108
15. Ginsberg M, Dietrich W, Busto R. Coupled forebrain increases of local cerebral glucose utilization and blood flow during physiologic stimulation of a somatosensory pathway in the rat. *Neurology* 1987;37:11–19
16. Reivich M, Sokoloff L, Kennedy C, Des Rosiers M. An autoradiographic method for the measurement of local glucose metabolism in the brain. In: Ingvar D, Lassen N, ed. *Brain Work*. Copenhagen: Munksgaard; 1975:377–384
17. Sokoloff L, Kety S. Regulation of cerebral circulation. *Physiol Rev* 1960;40:38–44
18. Roland P. *Brain Activation*. New York: Wiley-Liss, Inc; 1993
19. Leenders K, Perani D, Lammertsma A, et al. Cerebral blood flow, blood volume and oxygen utilisation: normal values and effect of age. *Brain* 1990;113:27–48